


Research Article

Detrital Zircon U-Pb-Hf Isotopes of Middle Neoproterozoic Sedimentary Rocks in the Altyn Tagh Orogen, Southeastern Tarim: Insights for a Tarim-South China-North India Connection in the Periphery of Rodinia

Qian Liu ^{1,2}, Guochun Zhao,^{3,4} Jianhua Li,⁵ Jinlong Yao,⁴ Yigui Han,⁴ Peng Wang,³ and Toshiaki Tsunogae^{2,6}

¹International Research Fellow of Japan Society for the Promotion of Science, Chiyoda-ku, Tokyo 102-0083, Japan

²Graduate School of Life and Environmental Sciences, The University of Tsukuba, Ibaraki 305-8572, Japan

³Department of Earth Sciences, The University of Hong Kong, Pokfulam Road, Hong Kong, China

⁴Department of Geology, Northwest University, Xi'an 710069, China

⁵China Institute of Geomechanics, Chinese Academy of Geological Sciences, Beijing 100081, China

⁶Department of Geology, University of Johannesburg, Auckland Park 2006, South Africa

Correspondence should be addressed to Qian Liu; niuniuliu880330@geol.tsukuba.ac.jp

Received 29 April 2020; Accepted 3 August 2020; Published 30 September 2020

Academic Editor: Alexander R. Simms

Copyright © 2020 Qian Liu et al. Exclusive Licensee GeoScienceWorld. Distributed under a Creative Commons Attribution License (CC BY 4.0).

The location of the Tarim craton during the assembly and breakup of the Rodinia supercontinent remains enigmatic, with some models advocating a Tarim-Australia connection and others a location at the heart of the unified Rodinia supercontinent between Australia and Laurentia. In this study, our new zircon U-Pb dating results suggest that middle Neoproterozoic sedimentary rocks in the Altyn Tagh orogen of the southeastern Tarim craton were deposited between ca. 880 and 760 Ma in a rifting-related setting slightly prior to the breakup of Rodinia at ca. 750 Ma. A compilation of existing Neoproterozoic geological records also indicates that the Altyn Tagh orogen of the southeastern Tarim craton underwent collision at ca. 1.0-0.9 Ga and rifting at ca. 850-600 Ma related to the assembly and breakup of Rodinia. Furthermore, in order to establish the paleoposition of the Tarim craton with respect to Rodinia, available detrital zircon U-Pb ages and Hf isotopes from Meso- to Neoproterozoic sedimentary rocks were compiled. Comparable detrital zircon ages (at ca. 0.9, 1.3-1.1, and 1.7 Ga) and Hf isotopes indicate a close linkage among rocks of the southeastern Tarim craton, Cathaysia, and North India but exclude a northern or western Australian affinity. In addition, detrital zircons from the northern Tarim craton exhibit a prominent age peak at ca. 830 Ma with minor spectra at ca. 1.9 and 2.5 Ga but lack Mesoproterozoic ages, comparable to the northern and western Yangtze block. Together with comparable geological responses to the assembly and breakup of the Rodinia supercontinent, we offer a new perspective of the location of the Tarim craton between South China and North India in the periphery of Rodinia.

1. Introduction

Most paleomagnetic studies, in agreement with plume-related magmatic rocks and glacial intervals, support the placement of the Tarim craton to the north or west of Australia in Neoproterozoic reconstructions of Rodinia [1-4]. In contrast, some authors [5-7] argue for a “missing link” con-

figuration of the Tarim craton at the heart of the unified Rodinia supercontinent between Australia and Laurentia, based on early Neoproterozoic to early Ediacaran paleomagnetic and tectonostratigraphic data from the Tarim craton.

However, ca. 1.0-0.6 Ga magmatism along the northern margin of the Tarim craton [8, 9] is younger than Grenville-age (ca. 1.35-1.05 Ga) magmatism within the

Musgrave and Albany-Fraser blocks of western-central Australia [10, 11], challenging a Tarim-western Australia linkage (e.g., [3]). Furthermore, ca. 1.0-0.6 Ga magmatic rocks from the northern Tarim craton have recently been reinterpreted to correlate with a long-lived subduction event [8, 9]. Such subduction-related magmatism without any Grenville-age unconformity or metamorphism indicates that the Tarim craton was probably located in the periphery of Rodinia with its northern margin facing the circum-Rodinia subduction zones [8, 9], rather than at the heart of Rodinia [6, 7]. In addition, the recognition of ca. 940-900 Ma syncollisional magmatism and metamorphism from the Altyn Tagh orogen of the southeastern Tarim craton supports to interpret that this orogen is the suture between the Tarim craton and another block during the amalgamation of Rodinia (e.g., [12–16]). However, the location of the Tarim craton in the periphery of Rodinia remains enigmatic and subsequent dispersal of the Tarim craton from Rodinia is not fully understood.

This study first reports on middle Neoproterozoic sedimentary rocks of the Altyn Tagh orogen of the southeastern Tarim craton, which were probably deposited in a rifting-related setting slightly earlier than the breakup of Rodinia due to the opening of the Proto-Tethys Ocean at ca. 750 Ma (e.g., [3, 17]). We suggest the placement of the Tarim craton between South China and North India with respect to Rodinia, based on a comparison of available detrital zircon age spectra and Hf isotope compositions.

2. Geological Background

The Altyn Tagh orogen occupies a crucial junction between the Tarim craton to the northwest, the Qilian orogen to the northeast, and the Qiadam block and the East Kunlun orogen to the southeast (Figure 1(a)). It has generally been divided into four units. From northeast to southwest, namely, the North Altyn Tagh terrane, the North Altyn Tagh subduction-accretion belt, the Central Altyn Tagh terrane, and the South Altyn Tagh subduction-collision belt (Figure 1(b)). The North Altyn Tagh terrane consists mainly of ca. 2.8 Ga and ca. 2.4-1.8 Ga orthogneiss and ca. 1.9 Ga paragneiss [5, 18] comparable to Archean to Paleoproterozoic basement of the Tarim craton [9]. The North Altyn Tagh subduction-accretion belt has been interpreted to represent an early Paleozoic accretionary orogenic system [19]. It consists mainly of ca. 520-450 Ma ophiolitic mélanges [20–22], ca. 512-491 Ma high-pressure (HP)/low-temperature (LT) eclogite and blueschist [23], ca. 514-390 Ma magmatic rocks [24–26], and early Paleozoic volcanosedimentary sequences [27]. In addition, the Suolak Formation containing ca. 760-750 Ma basalt and rhyolite associations are sporadically exposed in the North Altyn Tagh subduction-accretion belt [28, 29]. The Central Altyn Tagh terrane is composed of Meso- to Neoproterozoic metasedimentary rocks, ca. 920 Ma foliated rhyolite, ca. 754 Ma basalt, ca. 703 Ma A-type granite, and ca. 522-433 Ma intermediate to felsic magmatic rocks (Figure 1(c); [16, 25, 28, 30–32]). The South Altyn Tagh subduction-collision belt (Figure 1(b)), regarded as an early Paleozoic collisional orogenic system [19], is dominated

by ca. 501 Ma ophiolitic mélangé [33], ca. 508-475 Ma (U)HP and ca. 457-436 Ma Barrovian-type metamorphic rocks (e.g., [34–36]), and ca. 517-226 Ma magmatic rocks [25, 31]. Additionally, Meso- to Neoproterozoic metasedimentary rocks, ca. 940-900 Ma granitic rocks with I- and S-type affinities [12, 14], and ca. 763 Ma mafic rocks are recorded in the South Altyn Tagh subduction-collision belt (Figure 1(c)).

3. Sample Descriptions and Results

Sample 17LQ50-1A (GPS: 39°04'40.82"N, 92°15'09.67"E) was collected from an outcrop located ~8 km southwest of the main body of the Lapeiquan ophiolitic mélangé in the North Altyn Tagh subduction-accretion belt (Figures 1(a) and 2(a)).

The sampled outcrop contains rock associations of phyllite and quartz schist with prevailing cleavage and foliation (Figure 2(b)). It is associated with early Paleozoic sedimentary sequences in the matrix of the Lapeiquan ophiolitic mélangé (Figure 2(a)). Due to the poor quality of the outcrop, the relationship of this outcrop with early Paleozoic sedimentary sequences was difficult to establish in the field. Nonetheless, a tectonic contact is inferred (Figure 2(a)), based on (1) the strikingly distinctive rock associations of the studied schists and the conglomerate-sandstone beds of the early Paleozoic sedimentary sequences [27], (2) the different dip angles of the schistosity of the studied schists and the bedding of the early Paleozoic sedimentary sequences (Figure 2(a)), and (3) the extensive fault activities in the region (Figure 2(a)). Sample 17LQ50-1A is a fine-grained quartz schist. Major mineral compositions include elongated quartz (80%) and tiny muscovite (20%), which delineate well-developed schistosity (Figure 2(c)).

Detrital zircons extracted from sample 17LQ50-1A show subhedral, subrounded, and well-rounded forms with aspect ratios of 1-3 (Figure 3). They illustrate predominantly oscillatory zoning and subordinately homogeneous internal structures under cathodoluminescence (CL; Figure 3). Th (2-1926 ppm) and U (12-2765 ppm) contents are conspicuously variable with Th/U ratios of mostly >0.2 (Table DR1 in the GSA Data Repository (GSA Data Repository item 201Xxxx, analytical methods and results (Tables DR1 and DR2) and compiled data (Table DR3) are available online at <http://www.geosociety.org/pubs/ft20XX.htm> or on request from editing@geosociety.org)), indicative of a magmatic origin. Only six analytical spots have low Th/U ratios of 0.01-0.10 (Table DR1 in the GSA Data Repository), reflecting their metamorphic origin, as also indicated by their complex, heterogeneous CL images (Figure 3). For <1000 Ma and >1000 Ma zircons, the $^{206}\text{Pb}/^{238}\text{U}$ and $^{207}\text{Pb}/^{206}\text{Pb}$ ages were adopted, respectively. One analysis with an unreasonable minus error was deleted for discussion (Table DR1 in the GSA Data Repository). Another 140 measurements yielded a large variation of concordant Precambrian ages ranging from ca. 2700 to 888 Ma, characterized by a continuous age distribution of ca. 1.7-0.9 Ga and minor age abundances at ca. 2.7 and 2.0-1.9 Ga (Figure 3). The youngest zircon grain gave a concordant $^{206}\text{Pb}/^{238}\text{U}$ age of 888 ± 7 Ma, interpreted as the maximum

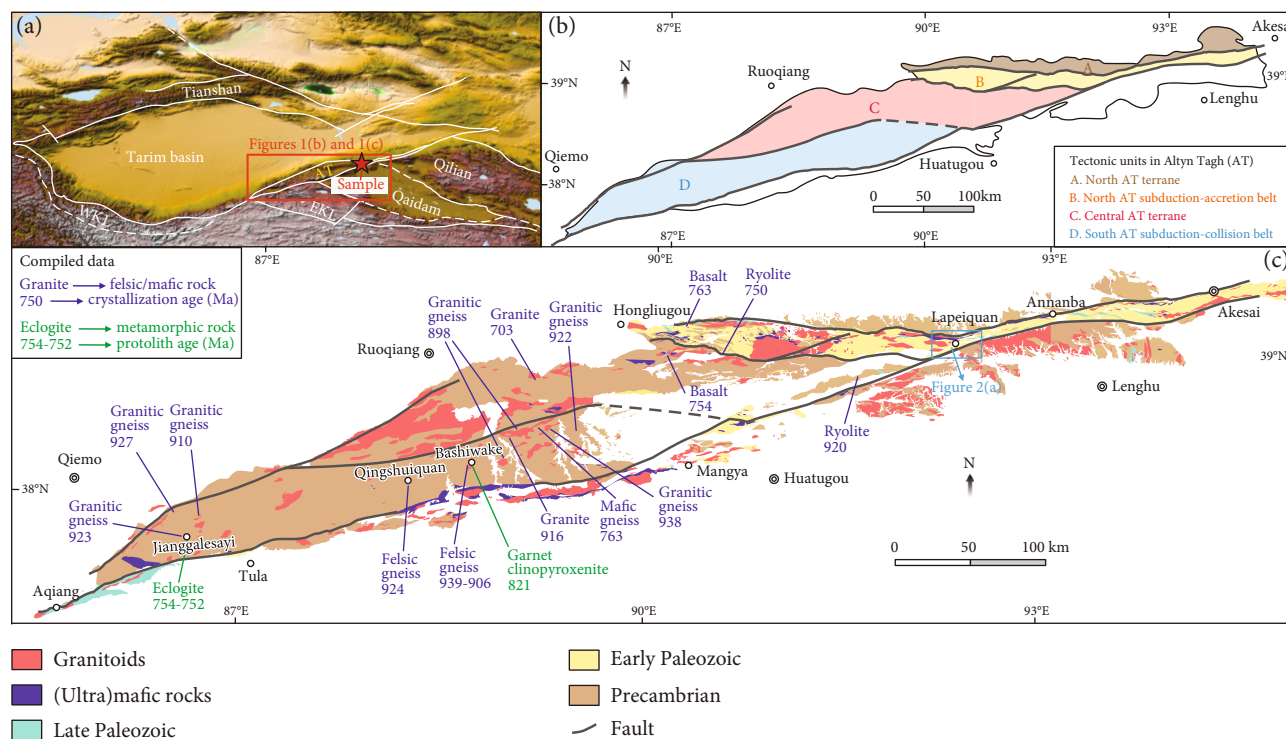


FIGURE 1: (a) Topographic map (from website <http://www.ngdc.noaa.gov/mgg/global/>) and location of the Altyn Tagh orogen and adjoining regions (modified from [5]). AT: Altyn Tagh; WKL: West Kunlun; EKL: East Kunlun. (b) Tectonic division of the Altyn Tagh orogen (modified after [34, 37]). (c) Detailed geological map of the Altyn Tagh orogen showing compiled ages of Neoproterozoic magmatic rocks and protoliths of metamorphic rocks (modified after [38–47]). Crystallization ages of magmatic rocks are from Wang et al. [12, 13], Wang [32], Zhang et al. [15, 16], Liu et al. [29], and Yu et al. [14]. Formation ages of protoliths of metamorphic rocks are from Liu et al. [34, 35, 48].

depositional age of sample 17LQ50-1A. Hf isotope analyses were carried out on 75 dated detrital zircons with a magmatic origin. Most detrital zircons exhibit a large spread of $\epsilon_{\text{Hf}}(t)$ values varying from -10 to +11, with only one grain aged ca. 902 Ma showing a highly negative $\epsilon_{\text{Hf}}(t)$ value of -15 (Figure 4; Table DR2 in the GSA Data Repository).

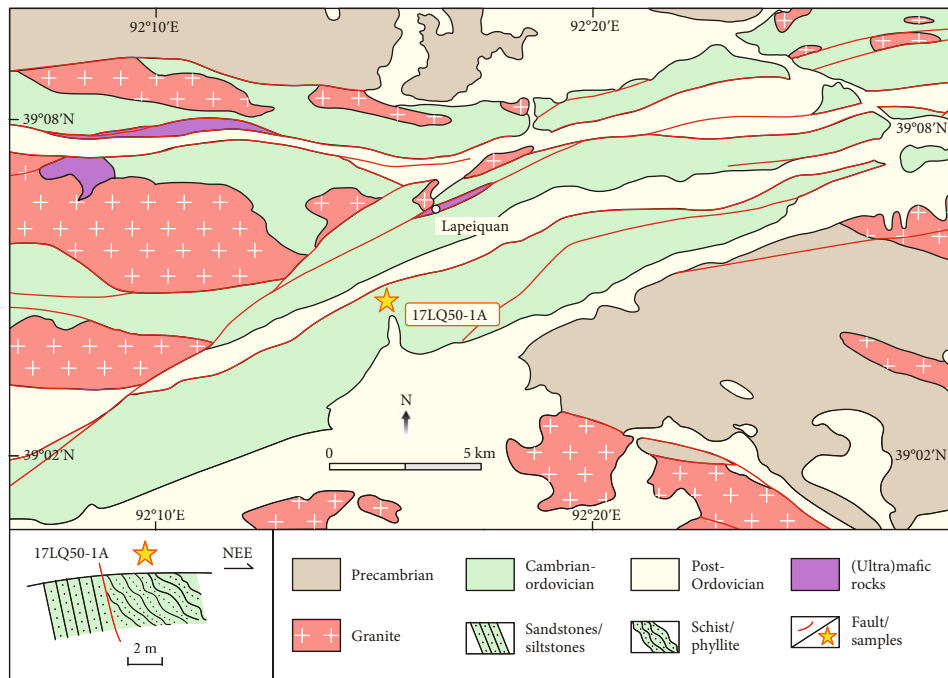
4. Depositional Age

The youngest zircon (888 ± 7 Ma) from sample 17LQ50-1A shows a subhedral, prismatic form with abraded edges (Figure 3), suggesting transportation before deposition to some extent. It indicates that sample 17LQ50-1A might have been deposited at some time posterior to ca. 888 Ma. In addition, the Suolak Formation of the North Altyn Tagh subduction-accretion belt [28, 29] provides a reliable estimate of its minimum age. The Suolak Formation consists of basalt, basaltic breccia and tuff, intermediate to felsic tuff, rhyolite, and chert, in which a SHRIMP zircon U-Pb age of ca. 763 Ma was obtained from a basalt [28] and a LA-ICP-MS zircon U-Pb age of ca. 750 Ma was obtained from a rhyolite [29]. The studied quartz schist is distinct from the volcanic and volcanoclastic sequences of the Suolak Formation (Figure 5) and does not contain any detrital zircons from the ca. 760–750 Ma volcanic rocks of the Suolak Formation [29]. Therefore, the studied sample was probably deposited earlier than the ca. 760–750 Ma Suolak Formation. In conclu-

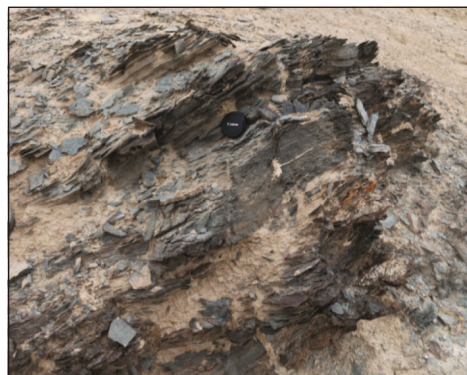
sion, sample 17LQ50-1A was probably deposited between ca. 880 and 760 Ma.

5. Geological Records of the Southeastern Tarim Craton in response to the Assembly and Breakup of Rodinia

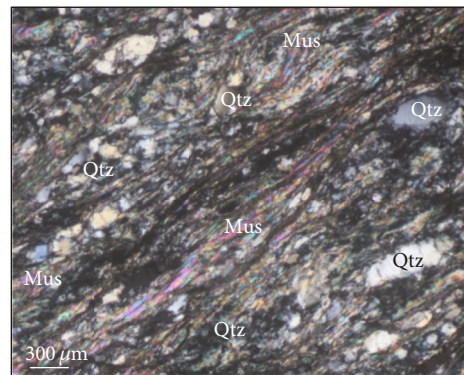
The main body of the Rodinia supercontinent finally assembled along major Grenvillian (ca. 1.3–1.0 Ma) orogenic belts in southern Laurentia, western and northern Australia, Amazonia, and the Maud-Namaqua-Natal Provinces of East Antarctica and Africa [10, 11, 56, 57]. In addition, ca. 1.0–0.9 Ga orogenic belts are documented in southwestern Baltica, the Eastern Ghats belt in India, and the Northern Prince Charles orogenic belt in East Antarctica [11, 56]. Such early Neoproterozoic tectonic events are also preserved in the Altyn Tagh orogen of the southeastern Tarim craton, as manifested by extensive ca. 940–900 Ma felsic magmatism in Central and South Altyn Tagh (Figure 1(c)). Geochemical studies revealed high-K calc-alkaline I-type and S-type affinities for the ca. 940–900 Ma granitic rocks and proposed an active continental margin [14] or a syncollisional setting [12]. A syncollisional regime is preferred based on ca. 910 Ma metamorphic zircon overgrowths on Mesoproterozoic zircon cores documenting in Mesoproterozoic metasedimentary rocks of the South Altyn Tagh subduction-collision belt [13]. It reflects metamorphism of Mesoproterozoic



(a)



(b)



(c)

FIGURE 2: (a) Geological map showing the sampling site and stratigraphic section of the Lapeiquan ophiolitic mélangé (modified after [46]). (b) Field photograph of phyllite and quartz schist in the sampled outcrop. (c) Photomicrograph (crossed nicols) of sample 17LQ50-1A. Qtz: quartz; Mus: muscovite.

supracrustal material at ca. 910 Ma [12], which was more likely related to syncollision. Recycling of Mesoproterozoic supracrustal material is also supported by ca. 1.9-1.4 Ga zircon Hf isotope model ages and coeval inherited zircon cores in some ca. 940-900 Ma granitic rocks [14, 15]. On the other hand, an active continental margin is also difficult to reconcile with the lack of typical arc-like products in the Altyn Tagh orogen, such as mafic-intermediate magmatic rocks and calc-alkaline granitoids. In addition, comparable ca. 1.0-0.9 Ga magmatic rocks are also distributed throughout the adjacent Qilian and Qaidam regions [14, 58]. Therefore, an early Neoproterozoic (ca. 1.0-0.9 Ga) collisional orogen characterizes the southeastern Tarim craton, which is coincident with the late assembly of the Rodinia supercontinent.

Following early Neoproterozoic final assembly, the interior of Rodinia underwent rifting-related extension at ca.

825-750 Ma, leading to the development of anorogenic magmatic rocks in most Rodinia terranes but not forming new oceans (e.g., [3]). The Rodinia supercontinent had not broken up until ca. 750-600 Ma due to the diachronous opening of relevant ocean domains [3, 17, 57]. Among these oceans, the Proto-Tethys Ocean separating Tarim, South China, and North China from other East Asian blocks was opened as early as ca. 750 Ma [3, 17]. Ca. 760-750 Ma basalt and rhyolite associations in the North Altyn Tagh subduction-accretion belt (Figure 1(c); [28, 29]) are coincident with the opening of the Proto-Tethys Ocean leading to the separation of the Tarim craton from Rodinia. The studied sample 17LQ50-1A deposited between ca. 880 and 760 Ma probably correlates with a rifting-related extensional setting prior to the separation of the Tarim craton from Rodinia. All these Neoproterozoic sedimentary and volcanic rocks of the North

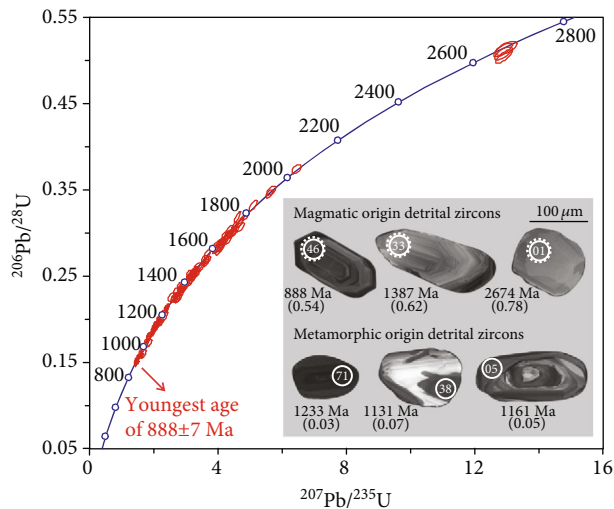


FIGURE 3: U-Pb concordia diagram and representative cathodoluminescence images of detrital zircons from sample 17LQ50-1A. The small solid and large dashed circles are locations for U-Pb dating and Hf isotope analyses, respectively. The numbers in the solid circles are analytical dot numbers. The values inside the brackets below U-Pb ages (Ma) are Th/U ratios.

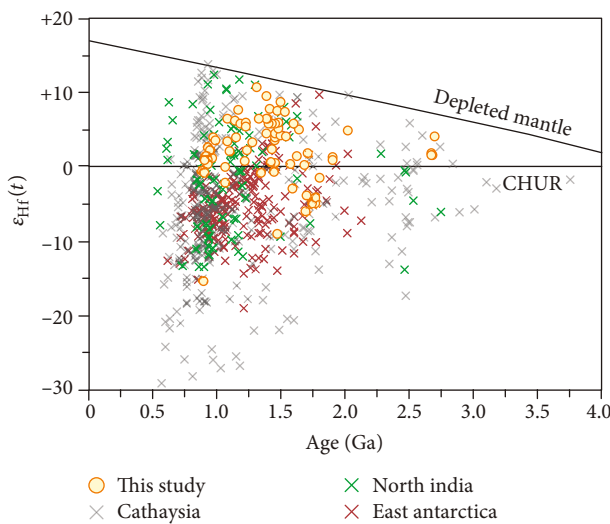


FIGURE 4: $\epsilon_{\text{Hf}}(t)$ values vs. U-Pb ages of detrital zircons from sample 17LQ50-1A. DM: depleted mantle; CHUR: chondrite. Comparative data from Cathaysia [49–52], North India [53, 54], and East Antarctica [55] are shown.

Altyn Tagh subduction-accretion belt were probably preserved in response to a well-preserved ca. 0.8–0.6 Ga rift depression throughout the Tarim basin [59]. Other geological records indicating middle-late Neoproterozoic extension in the Altyn Tagh orogen (Figure 1(c)) include ca. 763 Ma mafic rocks and ca. 703 Ma A-type granite in Central and South Altyn Tagh [15, 28, 32] and ca. 820–750 Ma MORB-like protoliths of the early Paleozoic eclogite and garnet peridotite in South Altyn Tagh [34, 35, 48]. Comparable ca. 800–600 Ma rifting-related mafic to felsic magmatism also operated throughout Qilian and Qaidam [60, 61]. Therefore,

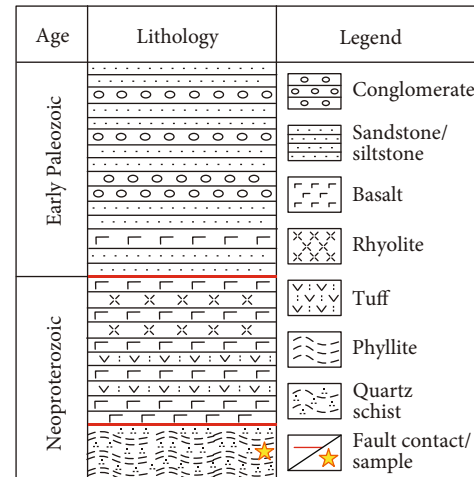


FIGURE 5: Stratigraphic column for Neoproterozoic to early Paleozoic strata in the matrix of the Lapeiquan ophiolitic mélangé (modified after [46]).

a middle-late Neoproterozoic (ca. 850–600 Ma) rifting regime was operating in the southeastern Tarim craton, associated with the extension and breakup of Rodinia.

In conclusion, the southeastern Tarim craton underwent ca. 1.0–0.9 Ga collision and ca. 850–600 Ma rifting in response to the assembly and breakup of Rodinia, respectively.

6. Linking Tarim with South China and North India during Rodinia

The ca. 2.7 Ga and ca. 2.0–1.9 Ga zircons from sample 17LQ50-1A are coincident with two episodes of granitic magmatism at ca. 2.8–2.3 Ga and ca. 2.0–1.8 Ga in the North Altyn Tagh terrane and the Tarim craton (e.g., [5, 18]), indicating a derivation from the Tarim basement. Similarly, the ca. 940–900 Ma felsic magmatic rocks in Central and South Altyn Tagh (Figure 1(c)) could be a potential source for the ca. 910 Ma detrital zircons in the studied sample. Some ca. 1497–1470 Ma diabase dikes were documented in the Kulu-ketage area of the northeastern Tarim craton [62, 63], but these mafic rocks might not have been the primary source material for the ca. 1.4 Ga detrital zircons in our studied sample because zircons typically crystallize from magmas with greater than 60% SiO₂ with much lesser abundance in lower silica magmas (e.g., [64]). Nonetheless, other source terranes that once connected with the southeastern Tarim craton during depositional time but subsequently drifted away were also required because ca. 1.7–1.1 Ga source rocks are lacking in the region. This highlights the importance of this study, in which we established the paleoposition of the Tarim craton within Rodinia by comparing available ages and Hf isotopes of detrital zircons from Meso- to Neoproterozoic sedimentary rocks in possible Rodinia terranes (Figures 4 and 6; Table DR3 in the GSA Data Repository).

A linkage between the southeastern Tarim craton and the Cathaysia block is suggested by comparable detrital zircon age populations at ca. 0.9, 1.3–1.1, and 1.7 Ga (Figure 6). The Cathaysia block exhibits variably negative to positive zircon $\epsilon_{\text{Hf}}(t)$ values at ca. 1.7 Ga, consistent with those of

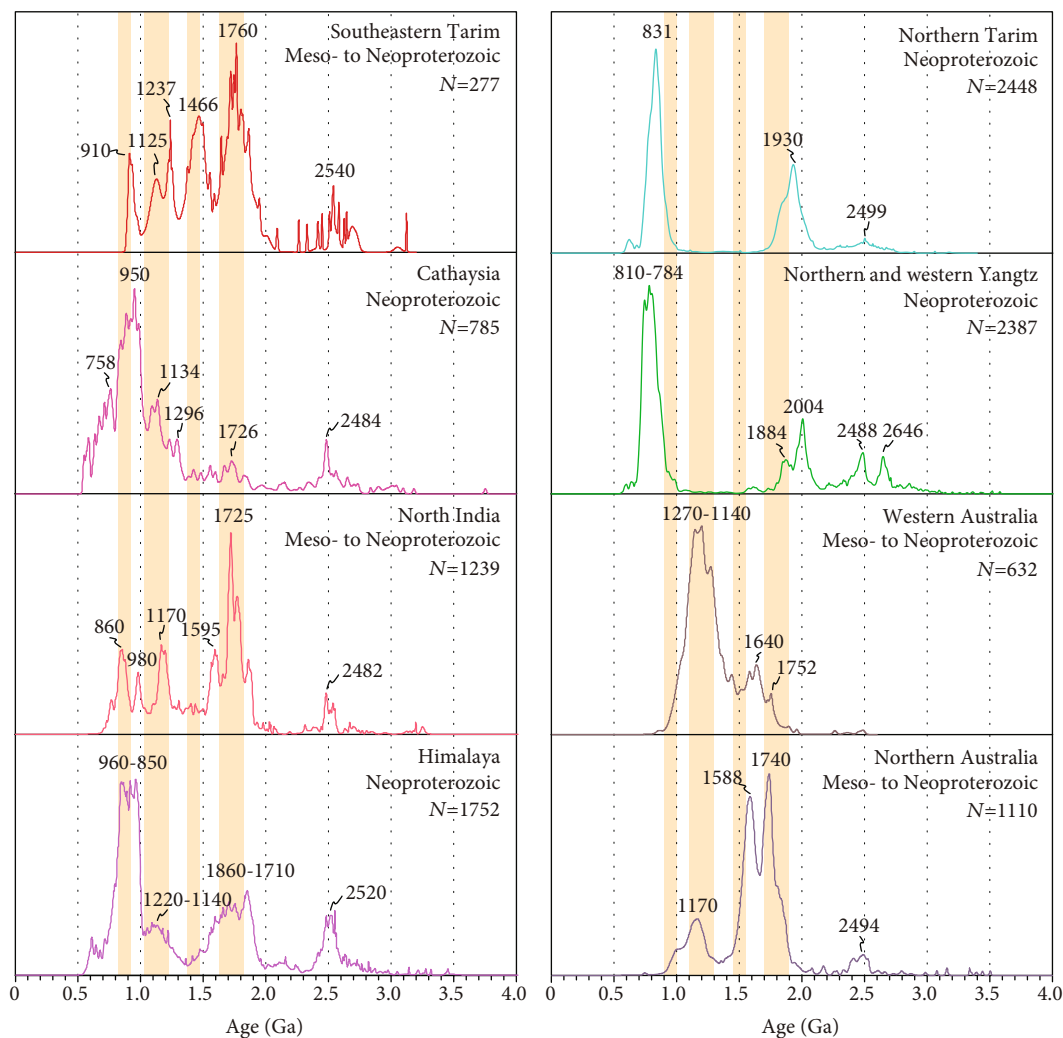


FIGURE 6: Probability curves for detrital zircon ages from the southeastern Tarim craton (this study; [18, 30]), the northern Tarim craton, and relevant Rodinia terranes (Table DR3 in the GSA Data Repository). N : number of analyses.

the coeval detrital zircons in the studied sample (Figure 4). Mostly positive $\varepsilon_{\text{Hf}}(t)$ values of the ca. 1.3-0.9 Ga detrital zircons in this study also agree with a large portion of the positive zircon $\varepsilon_{\text{Hf}}(t)$ values at ca. 1.3-0.9 Ga in Cathaysia (Figure 4). Notably, a zircon age peak at ca. 758 Ma in Cathaysia is absent in the southeastern Tarim craton because the studied sample was deposited prior to 760 Ma and unlikely contains such a young age peak at ca. 758 Ma. In addition, ca. 940-900 Ma collision operating within the southeastern Tarim craton is consistent with ca. 1.0-0.9 Ga collision recording in the Wuyi-Yunkai domains along southeastern Cathaysia (Figure 7; [52, 65]). The ca. 820-710 Ma sedimentation and bimodal magmatism due to the Nanhua rifting across South China [66–68] also matches well with the rifting-related records of the southeastern Tarim craton (see the above section).

A connection between the northern Tarim craton and the northern and western Yangtze block is indicated by the same prominent age spectrum at ca. 830 Ma and minor spectra at ca. 1.9 and 2.5 Ga of detrital zircons (Figure 6). Another age peak at ca. 2.6-2.7 Ga in the northern and western Yangtze

craton probably reflects the importance of ca. 2.6-2.7 Ga crystalline basement in the Yangtze craton [69, 70], which is relatively rare in the Tarim craton. Moreover, a ca. 1.0-0.6 Ga active continental margin along the northern Tarim craton [8, 9] is comparable to the ca. 1.0-0.7 Ga Panxi-Hannan belt along the northern and western peripheries of the Yangtze block [71, 72]. Together they probably belong to the Neoproterozoic accretionary orogen along the northern margin of Rodinia [9, 71, 73].

Collectively, a Tarim-South China linkage can be established in the periphery of Rodinia (Figure 7). South China was assembled by the connection of the Yangtze and Cathaysia blocks at ca. 820-800 Ma [68] and occupied a position adjacent to North India and western Australia with respect to Rodinia (Figure 7), based on comprehensive geologic, geochemical, geochronological, paleomagnetic, and faunal data [73]. We further suggest a location of the Tarim craton between South China and North India (Figure 7), according to the following lines of evidence.

First, a North Indian affinity for the southeastern Tarim craton is indicated by the similar age spectra (at ca. 1.2-0.9

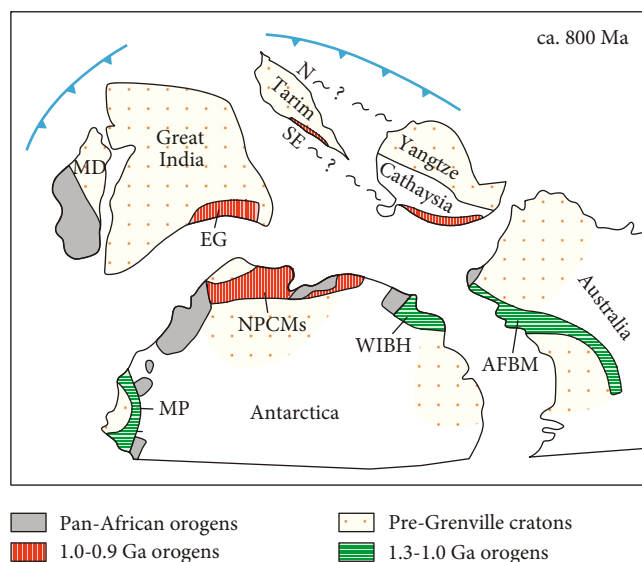


FIGURE 7: Location of the Tarim craton with respect to the Rodinia supercontinent at ca. 800 Ma (modified from [50, 52]). The wavy lines with “?” indicate possible linkages between the southeastern Tarim craton and the Cathaysia block and between the northern Tarim craton and the Yangtze block. SE: southeastern Tarim; N: northern Tarim; MD: Madagascar; EG: Eastern Ghats belt; NPCMs: Northern Prince Charles Mountains; MP: Maud Province; WIBH: Windmill Island/Bunger Hills; AFBM: Albany-Fraser belt/Musgrave block.

and 1.7 Ga) and $\epsilon_{\text{Hf}}(t)$ values for detrital zircons (Figures 4 and 6). This inference is also supported by the ca. 940–900 Ma collisional orogen in the southeastern Tarim craton, which is comparable to the ca. 990–900 Ma Eastern Ghats belt in India (Figure 7). In addition, the late Neoproterozoic strata in the Greater and Lesser Himalaya terranes were accumulated along the passive margin of North India [74, 75]. Their age spectra at ca. 1.2–0.9 and 1.7 Ga are consistent with our results (Figure 6), further demonstrating the close linkage between the southeastern Tarim craton and Great India (Figure 7). Furthermore, the ca. 1.4 Ga detrital zircons with positive $\epsilon_{\text{Hf}}(t)$ values in the studied sample were probably derived from the Northern Prince Charles Mountains of East Antarctica [11, 56] that exhibit a number of positive zircon $\epsilon_{\text{Hf}}(t)$ values at ca. 1.4 Ga (Figure 4).

Second, the ca. 1.0–0.6 Ga arc magmatic rocks along the northern Tarim craton are coeval with the ca. 1.0–0.8 Ga arc-related magmatic rocks of northwestern India and the ca. 800–720 Ma Andean-type arcs in the Seychelles and Madagascar [71, 76, 77], occupying the circum-Rodinia subduction-accretion system (Figure 7).

Third, we argue against an Australian affinity for the Tarim craton in the reconstruction of Rodinia [1, 2, 4]. The age spectra in this study are different from those in northern or southern Australia, which are characterized by a predominant age population at ca. 1.7–1.6 Ga but devoid of 0.9 and 1.4–1.3 Ga ages (Figure 6). A western Australian affinity is also questionable because western Australia lacks ca. 0.9 and 1.4 Ga detrital zircons from Meso- to Neoproterozoic sedimentary rocks (Figure 6). Importantly, even younger Permian sedimentary rocks in western Australia also lack ca. 0.9 and 1.4 Ga detrital zircons (e.g., [78]), implying coherent absence of ca. 0.9 and 1.4 Ga events in western Australia. In addition, the Grenvillian (ca. 1.3–1.0 Ga) orogens extending from the Albany-Fraser belt to the Musgrave block in western to central

Australia (Figure 7) are significantly older than the Neoproterozoic orogens in the peripheries of Tarim, challenging a western Australian affinity for the Tarim craton.

This study first reported middle Neoproterozoic sedimentary rocks in the Altyn Tagh orogen of the southeastern Tarim craton related to a rifting-related setting slightly earlier than the breakup of Rodinia at ca. 750 Ma. A new perspective on the location of the Tarim craton between South China and North India in the periphery of Rodinia is advocated based on Neoproterozoic geological records and detrital zircon U–Pb–Hf isotopes.

Data Availability

All data and analytical methods have been attached in Supplementary Materials.

Conflicts of Interest

The authors declare that they have no conflicts of interest.

Acknowledgments

This study was financially supported by a NSFC Project (41730213), Grant-in-Aids for Scientific Research from Japan Society for the Promotion of Science (JSPS) to Prof. Toshiaki Tsunogae (18H01300) and Dr. Qian Liu (No. 19F19020), and an open project from the State Key Laboratory for Mineral Deposits Research, Nanjing University (No. 21-16-03). JSPS International Research Fellowship is much appreciated. We appreciate the great help from Lei Wu, Jianfeng Gao, and Liang Li in experimental analyses.

Supplementary Materials

Table DR1: U-Pb dating results for detrital zircons from sample 17LQ50-1A and zircon standards GJ-1 and Plešovice. Table DR2: Hf isotope compositions of detrital zircons from sample 17LQ50-1A and zircon standards GJ-1, 91500, Plešovice, Mud Tank, and Penglai. Table DR3: compilation of detrital zircon ages from northern Tarim and relevant Rodinia blocks. Analytical methods. (*Supplementary Materials*)

References

- [1] Y. Chen, B. Xu, S. Zhan, and Y. Li, "First mid-Neoproterozoic paleomagnetic results from the Tarim Basin (NW China) and their geodynamic implications," *Precambrian Research*, vol. 133, no. 3-4, pp. 271–281, 2004.
- [2] B. Huang, B. Xu, C. Zhang, Y. a. Li, and R. Zhu, "Paleomagnetism of the Baiyisi volcanic rocks (ca. 740 Ma) of Tarim, Northwest China: a continental fragment of Neoproterozoic Western Australia?," *Precambrian Research*, vol. 142, no. 3-4, pp. 83–92, 2005.
- [3] Z. X. Li, S. V. Bogdanova, A. S. Collins et al., "Assembly, configuration, and break-up history of Rodinia: a synthesis," *Precambrian Research*, vol. 160, no. 1-2, pp. 179–210, 2008.
- [4] S. Zhan, Y. Chen, B. Xu, B. Wang, and M. Faure, "Late Neoproterozoic paleomagnetic results from the Sugetbrak Formation of the Aksu area, Tarim basin (NW China) and their implications to paleogeographic reconstructions and the snowball Earth hypothesis," *Precambrian Research*, vol. 154, no. 3-4, pp. 143–158, 2007.
- [5] S. Lu, H. Li, C. Zhang, and G. Niu, "Geological and geochronological evidence for the Precambrian evolution of the Tarim Craton and surrounding continental fragments," *Precambrian Research*, vol. 160, no. 1-2, pp. 94–107, 2008.
- [6] B. Wen, D. A. D. Evans, and Y.-X. Li, "Neoproterozoic paleogeography of the Tarim Block: An extended or alternative "missing-link" model for Rodinia?," *Earth and Planetary Science Letter*, vol. 458, pp. 92–106, 2017.
- [7] B. Wen, D. A. Evans, C. Wang, Y. X. Li, and X. Jing, "A positive test for the greater Tarim block at the heart of Rodinia: megadextral suturing of supercontinent assembly," *Geology*, vol. 46, no. 8, pp. 687–690, 2018.
- [8] R. F. Ge, W. B. Zhu, S. A. Wilde, J. W. He, X. Cui, and B. H. Zheng, "Neoproterozoic to Paleozoic long-lived accretionary orogeny in the northern Tarim Craton," *Tectonics*, vol. 33, no. 3, pp. 302–329, 2014.
- [9] Q. Liu, G. C. Zhao, M. Sun et al., "Ages and tectonic implications of Neoproterozoic ortho- and paragneisses in the Beishan Orogenic Belt, China," *China: Precambrian Research*, vol. 266, pp. 551–578, 2015.
- [10] D. J. Clark, B. J. Hensen, and P. D. Kinny, "Geochronological constraints for a two-stage history of the Albany–Fraser Orogen," *Western Australia: Precambrian Research*, vol. 102, pp. 155–183, 2000.
- [11] I. C. W. Fitzsimons, "Grenville-age basement provinces in East Antarctica: evidence for three separate collisional orogens," *Geology*, vol. 28, pp. 879–882, 2000.
- [12] C. Wang, L. Liu, Z. C. Che, D. L. Chen, A. D. Zhang, and J. H. Luo, "U–Pb geochronology and tectonic setting of the granitic gneiss in Jianggaleisayi Eclogite Belt, the Southern Edge of Altyn Tagh," *Geological Journal of Chin University*, vol. 12, pp. 74–82, 2006.
- [13] C. Wang, L. Liu, W. Q. Yang et al., "Provenance and ages of the Altyn Complex in Altyn Tagh: implications for the early Neoproterozoic evolution of northwestern China," *Precambrian Research*, vol. 230, pp. 193–208, 2013.
- [14] S. Y. Yu, J. X. Zhang, P. G. del Real et al., "The Grenvillian orogeny in the Altun–Qilian–North Qaidam mountain belts of northern Tibet Plateau: constraints from geochemical and zircon U–Pb age and Hf isotopic study of magmatic rocks," *Journal of Asian Earth Sciences*, vol. 73, pp. 372–395, 2013.
- [15] J. X. Zhang, H. K. Li, F. C. Meng, Z. Q. Xiang, S. Y. Yu, and J. P. Li, "Polyphase tectonothermal events recorded in metamorphic basement from the Altyn Tagh, the southeastern margin of the Tarim basin, western China: constraint from U–Pb zircon geochronology," *Acta Petrologica Sinica*, vol. 27, pp. 23–46, 2011.
- [16] Z. C. Zhang, Z. J. Guo, Z. S. Feng, and J. F. Li, "SHRIMP U–Pb age of zircons from Suoerkuli rhyolite in the Altyn Tagh mountains and its geological significations," *Acta Petrologica Sinica*, vol. 26, pp. 597–606, 2010.
- [17] G. C. Zhao, Y. J. Wang, B. C. Huang et al., "Geological reconstructions of the east Asian blocks: from the breakup of Rodinia to the assembly of Pangea," *Earth-Science Review*, vol. 186, pp. 262–286, 2018.
- [18] G. E. Gehrels, A. Yin, and X. F. Wang, "Detrital-zircon geochronology of the northeastern Tibetan plateau," *Geological Society of America Bulletin*, vol. 115, no. 7, pp. 881–896, 2003.
- [19] J. X. Zhang, S. Y. Yu, Y. S. Li, X. X. Yu, Y. H. Lin, and X. H. Mao, "Subduction, accretion and closure of Proto-Tethyan Ocean: Early Paleozoic accretion/collision orogeny in the Altun–Qilian–North Qaidam orogenic system," *Acta Petrologica Sinica*, vol. 31, pp. 3531–3554, 2015.
- [20] J. S. Yang, R. D. Shi, C. L. Wu et al., "Petrology and SHRIMP age of the Hongliugou ophiolite at Milan, north Altun, at the northern margin of the Tibetan plateau," *Acta Petrologica Sinica*, vol. 24, pp. 1567–1584, 2008.
- [21] Z. J. Yang, H. D. Ma, Z. X. Wang, and W. F. Xiao, "SHRIMP U–Pb zircon dating of gabbro from the Binggou ophiolite mélange in the northern Altyn, and geological implication," *Acta Petrologica Sinica*, vol. 28, pp. 2269–2276, 2012.
- [22] Z. C. Zhang, Z. J. Guo, and B. Song, "SHRIMP zircon dating of gabbro from the ophiolite mélange in the northern Altyn Tagh and its geological implications," *Acta Petrologica Sinica*, vol. 25, pp. 568–576, 2009.
- [23] J. X. Zhang, F. C. Meng, S. Y. Yu, W. Chen, and S. Y. Chen, "³⁹Ar–⁴⁰Ar geochronology of high-pressure/low-temperature blueschist and eclogite in the North Altyn Tagh and their tectonic implications," *Geology in China*, vol. 34, pp. 558–564, 2007.
- [24] B. L. Chen, S. B. Li, R. B. Jiang et al., "Zircon SHRIMP U–Pb dating of intermediate-felsic volcanic rocks from the Kaladawan area, Altun Mountains and its tectonic environment," *Acta Geologica Sinica*, vol. 90, pp. 708–727, 2016.
- [25] E. Cowgill, A. Yin, T. M. Harrison, and W. X. Feng, "Reconstruction of the Altyn Tagh fault based on U–Pb geochronology: role of back thrusts, mantle sutures, and heterogeneous crustal strength in forming the Tibetan Plateau," *Journal of Geophysical Research: Solid Earth*, vol. 108, no. B7, 2003.
- [26] L. T. Meng, B. L. Chen, N. N. Zhao et al., "The distribution, geochronology and geochemistry of early Paleozoic granitoid

- plutons in the North Altun orogenic belt, NW China: implications for the petrogenesis and tectonic evolution,” *Lithos*, vol. 268-271, pp. 399–417, 2017.
- [27] Q. Liu, G. C. Zhao, J. H. Li et al., “Provenance of early Paleozoic sedimentary rocks in the Altyn Tagh orogen: insights into the paleo-position of Tarim in Northern Gondwana associated with final closure of the Proto-Tethys Ocean,” *Geological Society of America Bulletin*, 2020.
- [28] GSIX (Geological Survey Institute of Xinjiang Uygur Autonomous Region), *Geological Map of the Kuoshibulak Area*, GSIX, Xinjiang, China, 2009, scale 1:50,000.
- [29] L. Liu, C. Wang, Y. T. Cao et al., “Geochronology of multi-stage metamorphic events: constraints on episodic zircon growth from the UHP eclogite in the South Altyn, NW China,” *Lithos*, vol. 136-139, pp. 10–26, 2012.
- [30] G. Gehrels, P. Kapp, P. DeCelles et al., “Detrital zircon geochronology of pre-tertiary strata in the Tibetan-Himalayan orogen,” *Tectonics*, vol. 30, no. 5, p. 30, 2011.
- [31] J. H. Liu, L. Liu, Y. S. Gai et al., “Zircon U-Pb dating and Hf isotopic compositions of the Baijianshan granodiorite in North Altyn Tagh and its geological significance,” *Acta Geologica Sinica*, vol. 91, pp. 1022–1038, 2016.
- [32] C. Wang, *Precambrian tectonic of south margin of Tarim Basin*, [Ph.D. thesis], Chin, Northwest University, NW China, 2011.
- [33] X. M. Li, Z. P. Ma, J. M. Sun et al., “Characteristics and age study about the Yuemakeqi mafic-ultramafic rock in the southern Altyn fault,” *Acta Petrologica Sinica*, vol. 25, pp. 862–872, 2009.
- [34] H. Liu, G. C. Wang, S. Z. Cao, Y. J. Luo, R. Gao, and W. X. Huang, “Discovery of Nanhuaian bimodal volcanics in northern Altyn Tagh and its tectonic significance,” *Earth Science—Journal of China University of Geosciences*, vol. 37, pp. 917–928, 2012.
- [35] L. Liu, A. D. Zhang, D. L. Chen, J. X. Yang, J. H. Luo, and C. Wang, “Implications based on LA-ICP-MS zircon U-Pb ages of eclogite and its country rock from Jianggalesayi area,” *Altyn Tagh: Earth Science Frontiers*, vol. 14, pp. 98–107, 2007.
- [36] J. X. Zhang, S. Y. Yu, and C. G. Mattinson, “Early Paleozoic polyphase metamorphism in northern Tibet, China,” *Gondwana Research*, vol. 41, pp. 267–289, 2017.
- [37] Y. Wu, *Compositions, structural deformation and geodynamics of the early paleozoic mélangé belt in North Altyn Tagh*, [Ph.D. thesis], Chinese Academy of Geological Science, China, 2016.
- [38] GBGP (Geological Bureau of Gansu Provincial), *Geological Map of the Subei Area*, Geological Publishing House, Beijing, 1976, scale 1:200,000.
- [39] GBGP (Geological Bureau of Gansu Provincial), *Geological Map of the Dangjinshankou and Duobagou Areas*, Geological Publishing House, Beijing, 1977, scale 1:200,000.
- [40] GBGP (Geological Bureau of Gansu Provincial), *Geological Map of the Lenghu Area*, Geological Publishing House, Beijing, 1979, scale 1:200,000.
- [41] IGHP (Institute of Geology and Mineral Resource of Henan Province), *Geological Map of the Suoerkuli and Bashikaogong Areas*, Geological Publishing House, Beijing, 1985, scale 1:200,000.
- [42] IGQP (Institute of Geology and Mineral Resource of Qinghai Province), *Geological Map of the Mangya Area*, Geological Publishing House, Beijing, 1984, scale 1:200,000.
- [43] IGQP (Institute of Geology and Mineral Resource of Qinghai Province), *Geological Map of the Eboliang Area*, Geological Publishing House, Beijing, 1986, scale 1:200,000.
- [44] RGGR (Regional Geological Survey Institute of Guangxi Zhuang Autonomous Region), *Geological Map of the Washixia and Altyn Tagh Areas*, RGGR, Guangxi, China, 2003, scale 1:250,000.
- [45] RGHP (Regional Geological Survey Institute of Hunan Province), *Geological Map of Aqiang-Qiemo County First Order Station*, RGHP, Hunan, China, 2003, scale 1:250,000.
- [46] TIMR (Tianjin Institute of Geology and Mineral Resource), *Geological Map of the Asbestos Ore*, TIMR, Tianjin, China, 2007, scale 1:250,000.
- [47] XCGS (Xi’an Center of Geological Survey, China Geological Survey), *Geological Map of the Bashikuergan Area*, XCGS, Xi’an, China, 2012, scale 1:250,000.
- [48] L. Liu, C. Wang, D. L. Chen, A. D. Zhang, and J. G. Liou, “Petrology and geochronology of HP–UHP rocks from the South Altyn Tagh, northwestern China,” *Journal of Asian Earth Science*, vol. 35, no. 3-4, pp. 232–244, 2009.
- [49] L. M. Li, M. Sun, Y. J. Wang et al., “U–Pb and Hf isotopic study of detrital zircons from the meta-sedimentary rocks in central Jiangxi Province, South China: implications for the Neoproterozoic tectonic evolution of South China block,” *Journal of Asian Earth Sciences*, vol. 41, no. 1, pp. 44–55, 2011.
- [50] W. Wang, M. F. Zeng, M. F. Zhou, J. H. Zhao, J. P. Zheng, and D. F. Zeng, “Age, provenance and tectonic setting of Neoproterozoic to early Paleozoic sequences in southeastern South China Block: constraints on its linkage to western Australia-East Antarctica,” *Precambrian Research*, vol. 309, pp. 290–308, 2018.
- [51] J. H. Yu, S. Y. O’Reilly, L. J. Wang et al., “Components and episodic growth of Precambrian crust in the Cathaysia Block, South China: evidence from U–Pb ages and Hf isotopes of zircons in Neoproterozoic sediments,” *Precambrian Research*, vol. 181, no. 1-4, pp. 97–114, 2010.
- [52] J. H. Yu, S. Y. O’Reilly, L. J. Wang et al., “Where was South China in the Rodinia supercontinent?: evidence from U–Pb geochronology and Hf isotopes of detrital zircons,” *Precambrian Research*, vol. 164, pp. 1–15, 2008.
- [53] W. Wang, P. A. Cawood, M. K. Pandit, X. P. Xia, and J. H. Zhao, “Coupled Precambrian crustal evolution and supercontinent cycles: Insights from in-situ U–Pb, O- and Hf-isotopes in detrital zircon, NW India,” *American Journal of Science*, vol. 318, pp. 989–1017, 2018.
- [54] D. C. Zhu, Z. D. Zhao, Y. L. Niu, Y. Dilek, and X. X. Mo, “Lhasa terrane in southern Tibet came from Australia,” *Geology*, vol. 39, no. 8, pp. 727–730, 2011.
- [55] X. C. Liu, Y. Zhao, H. Chen, and B. Song, “New zircon U–Pb and Hf–Nd isotopic constraints on the timing of magmatism, sedimentation and metamorphism in the northern Prince Charles Mountains, East Antarctica,” *Precambrian Research*, vol. 299, pp. 15–33, 2017.
- [56] S. D. Boger, C. J. Carson, C. J. L. Wilson, and C. M. Fanning, “Neoproterozoic deformation in the Radok Lake region of the northern Prince Charles Mountains, east Antarctica; evidence for a single protracted orogenic event,” *Precambrian Research*, vol. 104, no. 1-2, pp. 1–24, 2000.
- [57] P. A. Cawood, A. A. Nemchin, R. Strachan, T. Prave, and M. Krabbendam, “Sedimentary basin and detrital zircon record along East Laurentia and Baltica during assembly and

- breakup of Rodinia,” *Journal of the Geological Society*, vol. 164, no. 2, pp. 257–275, 2007.
- [58] K. A. Tung, H. Y. Yang, D. Y. Liu et al., “The amphibolite-facies metamorphosed mafic rocks from the Maxianshan area, Qilian block, NW China: a record of early Neoproterozoic arc magmatism,” *Journal of Asian Earth Science*, vol. 46, pp. 177–189, 2012.
- [59] B. Z. He, C. L. Jiao, T. Z. Huang et al., “Structural architecture of Neoproterozoic rifting depression groups in the Tarim Basin and their formation dynamics,” *Science China: Earth Sciences*, vol. 62, no. 3, pp. 529–549, 2019.
- [60] C.-Y. Tseng, H.-Y. Yang, W. Yusheng et al., “Finding of Neoproterozoic (~775 Ma) magmatism recorded in metamorphic complexes from the north Qilian orogen: evidence from SHRIMP zircon U-Pb dating,” *Chinese Science Bulletin*, vol. 51, no. 8, pp. 963–970, 2006.
- [61] X. Xu, S. G. Song, L. Su, Z. X. Li, Y. L. Niu, and M. B. Allen, “The 600–580Ma continental rift basalts in North Qilian Shan, northwest China: links between the Qilian-Qaidam block and SE Australia, and the reconstruction of East Gondwana,” *Precambrian Research*, vol. 257, pp. 47–64, 2015.
- [62] X. D. Wang, X. B. Lv, X. F. Cao, Y. F. Wang, and W. Liu, “Palaeo-Mesoproterozoic magmatic and metamorphic events from the Kuluketage block, northeast Tarim Craton: geochronology, geochemistry and implications for evolution of Columbia,” *Geological Journal*, vol. 53, pp. 120–138, 2017.
- [63] C. Z. Wu, M. Santosh, Y. J. Chen et al., “Geochronology and geochemistry of Early Mesoproterozoic meta-diabase sills from Quruqtagh in the northeastern Tarim Craton: implications for breakup of the Columbia supercontinent,” *Precambrian Research*, vol. 241, pp. 29–43, 2014.
- [64] P. A. Cawood, C. J. Hawkesworth, and B. Dhuime, “Detrital zircon record and tectonic setting,” *Geology*, vol. 40, no. 10, pp. 875–878, 2012.
- [65] Y. J. Wang, Y. Z. Zhang, W. M. Fan, H. Y. Geng, H. P. Zou, and X. W. Bi, “Early Neoproterozoic accretionary assemblage in the Cathaysia Block: Geochronological, Lu-Hf isotopic and geochemical evidence from granitoid gneisses,” *Precambrian Research*, vol. 249, pp. 144–161, 2014.
- [66] J. Wang and Z. X. Li, “History of Neoproterozoic rift basins in South China: implications for Rodinia break-up,” *Precambrian Research*, vol. 122, pp. 141–158, 2003.
- [67] Y. J. Xin, J. H. Li, S. W. Dong, Y. Q. Zhang, W. B. Wang, and H. S. Sun, “Neoproterozoic post-collisional extension of the central Jiangnan orogen: geochemical, geochronological, and Lu-Hf isotopic constraints from the ca. 820–800 Ma magmatic rocks,” *Precambrian Research*, vol. 294, pp. 91–110, 2017.
- [68] J. L. Yao, P. A. Cawood, L. S. Shu, and G. C. Zhao, “Jiangnan Orogen, South China: A ~970-820 Ma Rodinia margin accretionary belt,” *Earth-Science Review*, vol. 196, p. 102872, 2019.
- [69] K. Chen, S. Gao, Y. B. Wu et al., “2.6-2.7 Ga crustal growth in Yangtze craton, South China,” *Precambrian Research*, vol. 224, pp. 472–490, 2013.
- [70] J. Q. Wei, Y. X. Wei, J. X. Wang, and X. D. Wang, “Geochronological constraints on the formation and evolution of the Huangling basement in the Yangtze craton, South China,” *Precambrian Research*, vol. 342, p. 105707, 2020.
- [71] P. A. Cawood, G. C. Zhao, J. L. Yao, W. Wang, Y. J. Xu, and Y. J. Wang, “Reconstructing South China in phanerozoic and precambrian supercontinents,” *Earth-Science Review*, vol. 186, pp. 173–194, 2018.
- [72] Y. P. Dong, X. M. Liu, M. Santosh et al., “Neoproterozoic accretionary tectonics along the northwestern margin of the Yangtze Block, China: constraints from zircon U–Pb geochronology and geochemistry,” *Precambrian Research*, vol. 196–197, pp. 247–274, 2012.
- [73] P. A. Cawood, Y. J. Wang, Y. J. Xu, and G. C. Zhao, “Locating South China in Rodinia and Gondwana: a fragment of greater India lithosphere?,” *Geology*, vol. 41, pp. 903–906, 2013.
- [74] M. Hofmann, U. Linnemann, V. Rai, S. Becker, A. Gärtnera, and A. Sagawe, “The India and South China cratons at the margin of Rodinia—synchronous Neoproterozoic magmatism revealed by LA-ICP-MS zircon analyses,” *Lithos*, vol. 123, no. 1–4, pp. 176–187, 2011.
- [75] N. McQuarrie, D. Robinson, S. Long et al., “Preliminary stratigraphic and structural architecture of Bhutan: implications for the along strike architecture of the Himalayan system,” *Earth and Planetary Science Letter*, vol. 272, no. 1–2, pp. 105–117, 2008.
- [76] C. V. D. Rao, M. Santosh, S. W. Kim, and S. R. Li, “Arc magmatism in the Delhi Fold Belt: SHRIMP U–Pb zircon ages of granitoids and implications for Neoproterozoic convergent margin tectonics in NW India,” *Journal of Asian Earth Science*, vol. 78, pp. 83–99, 2013.
- [77] W. Wang, P. A. Cawood, M. F. Zhou, M. K. Pandit, X. P. Xia, and J. H. Zhao, “Low- $\delta^{18}\text{O}$ rhyolites from the Malani igneous suite: a positive test for south China and NW India linkage in Rodinia,” *Geophysical Research Letters*, vol. 44, pp. 10–298, 2017.
- [78] J. J. Veevers, A. Saeed, E. A. Belousova, and W. L. Griffin, “U–Pb ages and source composition by Hf-isotope and trace-element analysis of detrital zircons in Permian sandstone and modern sand from southwestern Australia and a review of the paleogeographical and denudational history of the Yilgarn craton,” *Earth-Science Reviews*, vol. 68, no. 3–4, pp. 245–279, 2005.